ARTICLE

Compact Metallo-Dielectric Optical Antenna for Ultra Directional and Enhanced Radiative Emission

Alexis Devilez, Brian Stout, and Nicolas Bonod*

Institut Fresnel, CNRS, Aix-Marseille Université, Ecole Centrale Marseille, Domaine Universitaire de Saint Jérôme, 13397 Marseille, France

ABSTRACT We report the design of highly efficient optical antennas employing a judicious synthesis of metallic and dielectric materials. In the proposed scheme, a pair of metallic coupled nanoparticles permits large enhancements in both excitation strength and radiative decay rates, while a high refractive index dielectric microsphere is employed to efficiently collect light without spoiling the emitter quantum efficiency. Our simulations indicate potential fluorescence rate enhancements of 3 orders of magnitude over the entire optical frequency range.

KEYWORDS: nanoantenna · single emitter · LSPRs · plasmons · colloidal lens

Photoluminescence signal detection of fluorescent molecules or quantum dots is a crucial issue in many photonic applications. The recent concept of optical nanoantennas is based on using plasmonic nanostructures to tailor the electromagnetic environment near a quantum emitter in order to enhance the photoluminescence signal by optimizing (a) the local excitation rate, (b) the emission rate, and (c) the collection efficiency.[1,2] During the past decade, several types of metallic nanostructures, in particular, coupled metallic particles[3−6] and subwavelength holes,[7,8] have demonstrated their ability to confine light in nanometer scale volumes and strongly enhance the excitation rate of single emitters placed in their vicinity.

Reciprocally, nanoscale metallic structuring modifies the local density of states,[9] thereby modifying the radiation properties of nearby photoemitters. Metallic structures introduce electromagnetic relaxation channels such as plasmonic modes that can strongly enhance the total decay rate.[10,11] However, due to their lossy nature, nonradiative relaxation rates can become preponderant when an emitter is located too close to a metallic structure.[12−19] This quenching effect can spoil the benefits of plasmon excitation. Consequently, it is crucially important in nanoantenna applications to determine the quantum efficiency, defined as the ratio between the radiative and total decay rates, particularly for small separations between the emitter and the metallic structure. Photoluminescence enhancement thus relies on a trade-off between excitation rate enhancements and high quantum efficiencies.[20]

Additionally, recent papers have addressed the important issue of the angular redistribution of radiated power induced by the structured local environment. Recently, the Yagi-Uda radio antenna has been successfully downscaled to the optical range to obtain high directionality of light radiation.[21−24] The high directionality obtained with these structures requires couplings between the emitted light and the plasmon modes, necessitating a rather large number of nanoparticles. The size of a metallic director can be reduced to two coupled nanoparticles[17,25] but at a price of a lower directivity. The design of an optical antenna based on a fully plasmonic approach is still challenging since high directionality can suffer from ohmic losses inherent to metallic structures and requires precise manufacturing techniques to align several particles. Dielectric materials have usually been disregarded in this context because their extinction cross sections are comparable in size to their geometrical cross section, thus producing weak excitation rates. However, it has been demonstrated that high refractive index dielectric materials can induce a redirection of the dipolar emission.[26−28] Arrays of dielectric nanoparticles have also shown their ability to redirect light.[29] The considerable advantage of transparent (lossless) dielectrics is that they preserve the quantum efficiency.

*Address correspondence to nicolas.bonod@fresnel.fr.

Received for review February 20, 2010 and accepted May 20, 2010.

Published online May 28, 2010.
10.1021/nn100348d

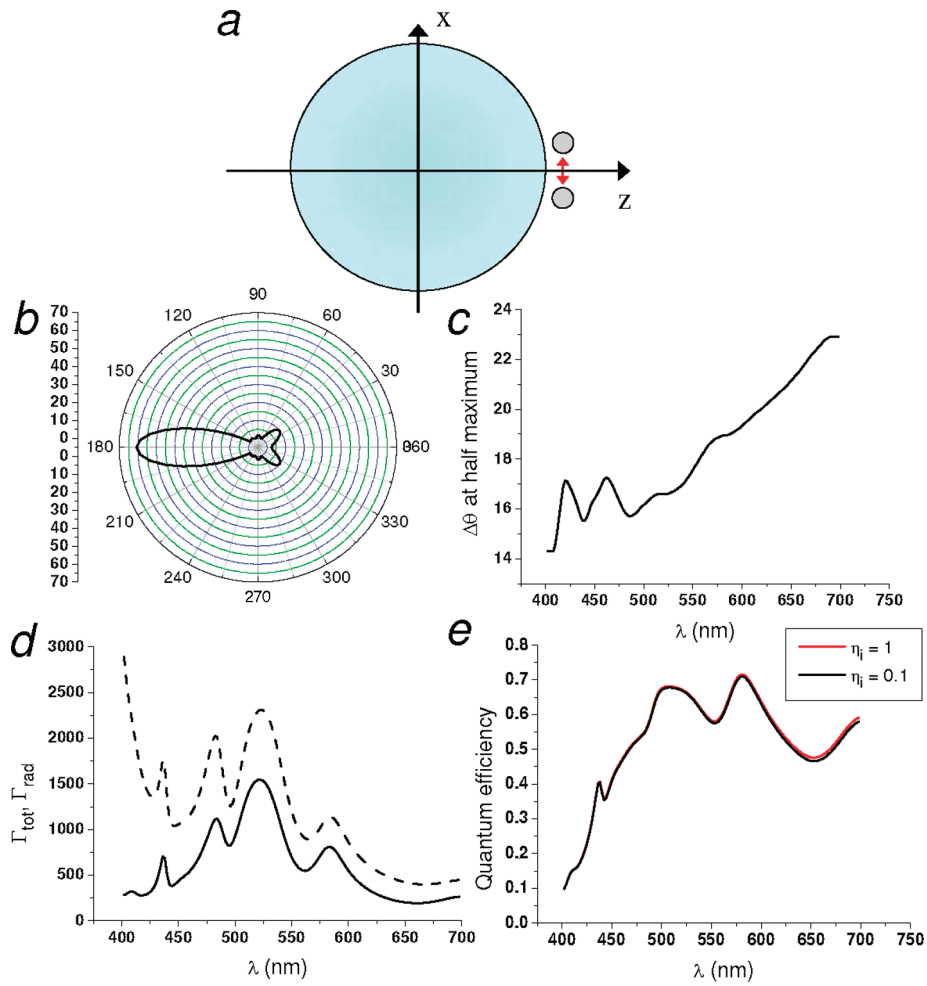

Figure 1. (a) Antenna schematic: a dielectric microsphere (D = 500 nm, n_{TiO_2} taken from Yamada *et al.*[33]) and two silver nanoparticles separated by 8 nm (D = 60 nm and n_{Ag} taken from Palik[34]) are embedded in a dielectric background of refractive index n_0 = 1.3. A dipolar emitter is placed equidistantly from the silver spheres along their axis of separation. (b) Radiation diagram at λ = 525 nm, (c) collection angle (3 dB half-width), (d) total (dashed line) and radiative (solid line) decay rate enhancements, and (e) quantum efficiency for a perfect emitter (red line) and a poor emitter, η_i = 0.1 (black line).

This work demonstrates that a judicious combination of dielectric and metallic materials can produce a highly directional compact optical antenna, which strongly enhances both local field excitation and radiation rate of a dipolar emitter. We will see that desirable properties occur in conjunction with a large quantum efficiency, thereby ensuring a high fluorescence emission rate.

In this article, numerical simulations are performed within the framework of rigorous Mie theory combined with a multiple scattering formulation.[30−32] The single emitter is simulated as a dipolar source modeled by taking the first electric term in a multipole (Mie) expansion. The generalized Lorentz−Mie calculations are performed with a truncation order of N = 20 for the individual scatterers. The total emitted power, P_{tot}, and the radiative emitted power, P_{rad}, are calculated by integrating the radial component of the Poynting vector over a spherical surface surrounding the source at respective distances of 1 nm and 5 μm. The total and radiative decay rate enhancements are then obtained by normalizing the emitted power in the presence of the antenna by the emitted power in the homogeneous background medium: $\Gamma_{tot} = P_{tot}/P_0$ and $\Gamma_{rad} = P_{rad}/P_0$. The quantum efficiency is then defined as

$$\eta = \frac{\Gamma_{rad}}{(\Gamma_{tot} + (1 - \eta_i)/\eta_i)} \qquad (1)$$

where η_i represents the intrinsic quantum efficiency of the emitter (η_i = 1 for a perfect emitter).

RESULTS AND DISCUSSION

The schematic of the antenna being considered is displayed in Figure 1a. The optical antenna consists of a TiO_2 dielectric microsphere[27,33] (D = 500 nm) and two silver nanospheres (D = 60 nm separated by 8 nm) embedded in a dielectric background of refractive index n_0 = 1.3. A dipolar-like source oriented along the x-axis is placed 30 nm from the dielectric microsphere and centered equidistantly along the axis joining the silver spheres. Figure 1b displays the radiation pattern of the antenna (polar plot of the radiated power per angle

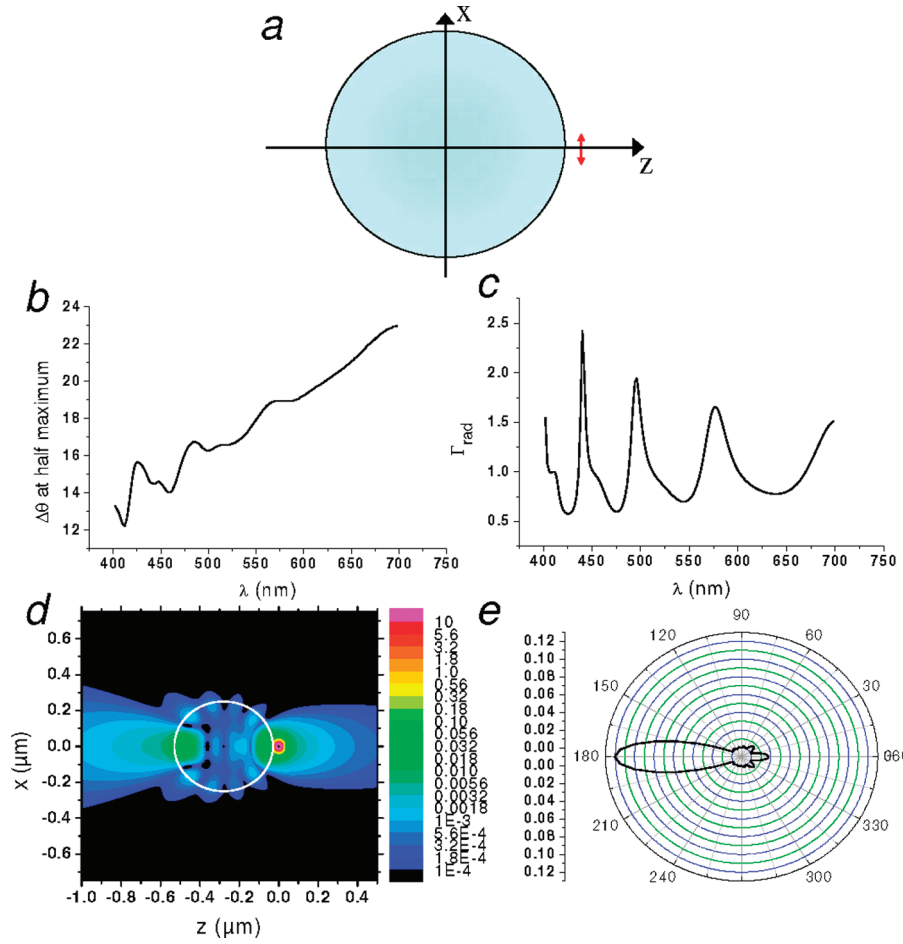

Figure 2. Characterization of a TiO_2 microsphere as an optical antenna. (a) Microsphere is embedded in a background medium of refractive index index $n_0 = 1.3$. The refractive index of TiO_2 is taken from ref 33, (b) collection angle (3 dB half-width), (c) radiative decay rate, (d) colored map of the electric field intensity, and (e) radiation diagram at $\lambda = 440$ nm.

unit) for a dipole oscillating at $\lambda = 525$ nm (λ is the wavelength in vacuum). Contrary to free space radiation, Figure 1b exhibits a highly directional emission with an angular aperture (3 dB half-width) $\simeq 15°$. Calculations displayed in Figure 1c show that the collection angle remains below 25° for a wavelength range from 400 to 700 nm. More interestingly, this highly directive radiation is concurrent with a strong enhancement of the radiative decay rate. The radiative decay rate enhancement (full line) displayed in Figure 1d surpasses 2 orders of magnitude over the entire optical frequency range. Moreover, the spectral feature of Γ_{rad} shows several peaks higher than 10^3, revealing electromagnetic structural resonances that will be attributed later to the excitation of cavity resonances occurring in the high refractive index microsphere. In other words, this optical antenna does not require an optimization of the electromagnetic resonances in order to be efficient, but an optimization of the electromagnetic couplings between the dipolar emitter and electromagnetic resonances permits radiative decay factors Γ_{rad} as high as 10^3. The high quality of the antenna is confirmed in Figure 1e, which shows a quantum efficiency greater than 0.5 for $\lambda > 450$ nm. Even more spectacularly, we remark that the quantum efficiency of a poor emitter (black line in Figure 1e) is essentially the same as the quantum efficiency of a perfect emitter (red line). Further calculations show that this property is fulfilled for any intrinsic quantum efficiency higher than 10^{-3}. This behavior is mainly due to the giant decay rates enhancements which render the term $(1 - \eta_i)/\eta_i$ in eq 1 negligible compared to Γ_{tot}.

In summary, this simple and compact system turns out to be a highly performant antenna over the entire optical spectrum and is characterized by a high directionality, strong decay rate enhancements, and a high quantum efficiency. In the remainder of this work, we investigate the properties of the dielectric and metallic components separately in order to better understand the unique performance of this optical antenna.

We first investigate the properties of a single high refractive index dielectric microsphere. Recent studies have demonstrated that dielectric microspheres operate as efficient near-field "lenses" with performances comparable to the state of art of high numerical aperture microscopes such as immersion lenses.[27,28,35−37] Figure 2b displays the angular 3 dB half-width of the emerging propagative beam produced by a dipole lo-

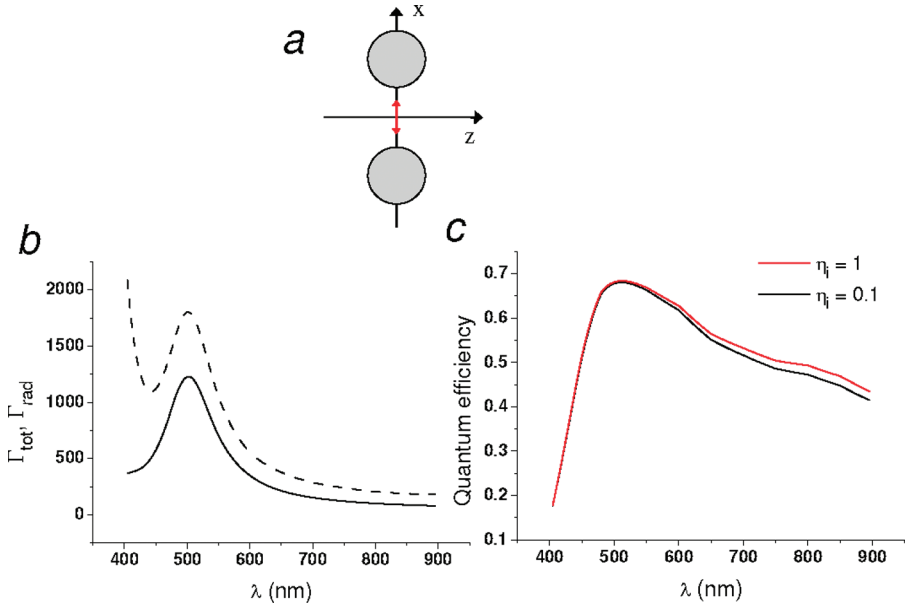

Figure 3. Characterization of the two silver nanoparticles (D = 60 nm) embedded in a dielectric background of refractive index n_0 = 1.3. The dipolar light source is set midway between the two metallic elements separated by 8 nm and is assumed to be oriented along the separation axis. Refractive index of silver is taken from ref 34. (b) Total (dashed line) and radiative (solid line) decay rate enhancements, (c) quantum efficiency for a perfect emitter (red line) and a poor emitter, η_i = 0.1 (black line) as a function of the wavelength.

cated at 30 nm from the sphere surface (the dipole is oriented along the *x*-axis). It clearly demonstrates that a single TiO_2 microsphere 500 nm in diameter can redirect dipolar radiated power into a narrow beam of 3 dB half-width below 25° over a large frequency bandwidth covering almost all of the optical range. Furthermore, the radiative decay rate enhancement displayed in Figure 2c shows several peaks in the spectrum with moderated amplitudes. This behavior feature might seem surprising at first since dielectric materials generally exhibit low enhancement of the radiative decay rates. However, let us recall that the high refractive index of TiO_2 enables the well-known electromagnetic resonances in the dielectric microsphere called whispering gallery modes (WGMs).[38,39] This assertion is clearly demonstrated in Figure 2d, which displays the electric field intensity in the vicinity of a dielectric microsphere dipole illuminated at λ = 440 nm corresponding to the narrowest peak in Figure 2c. Furthermore, the far-field radiation pattern of emitted light at λ = 440 nm (displayed in Figure 2e) demonstrates that the excitation of WGMs does not significantly deteriorate the strong directional properties of the TiO_2 microsphere illuminated by a dipole. The WGM resonances do, however, have the ability to slightly enhance the radiative decay rates of a dipolar emitter. In summary, high refractive dielectric spheres can serve as simple and compact optical antennas in a very wide range of frequencies. Nevertheless, the huge decay rates enhancements observed in Figure 1d cannot be explained by the coupling of a dipolar emitter with WGM resonances. One concludes therefore that the bulk of the decay rate enhancements of the metallo-dielectric antenna is due to the metallic materials in the near-field of the emitting dipole.

Coupled nanoparticles have been widely studied in the context of nanodimers[19,40] and bowtie nanoantennas[11,41] to enhance the radiative decay rate of a single emitter. Figure 3b displays the total (dashed line) and radiative (solid line) decay rate enhancements when a dipole oriented along the *x*-axis is set in the center of the cavity formed by two silver nanoparticles 60 nm in diameter separated by 8 nm. A broad peak appears corresponding to the well-known redshifted plasmon resonance of two coupled metallic particles.[4] Comparison between Figure 1c and Figure 2b shows that the so-called superemitter[10] does not significantly modify the radiation directionality when it is combined with a microsphere. As illustrated in Figure 3c, the presence of metallic losses induces a drop of the quantum efficiency of a perfect emitter (red line), particularly strong near-ultraviolet frequencies. Consequently, although the efficiency of a perfect emitter is decreased due to relaxation *via* nonradiative channels, the quantum efficiency of a poor emitter is increased several-fold (*cf.* Figure 3c with η_i = 0.1).

The design of optical antennas has been widely inspired by their analogues in the radio frequency range, the Yagi-Uda antenna in particular.[21−24] This antenna is typically made of three elements: the feed, the collector, and the reflector. The feed element role is to improve couplings between the emitter and the antenna. The optical analogue of the collector generally consists of several coupled metal particles acting as a guide for plasmon waves, while the reflector can be made from a slightly larger single metallic particle. In our proposed

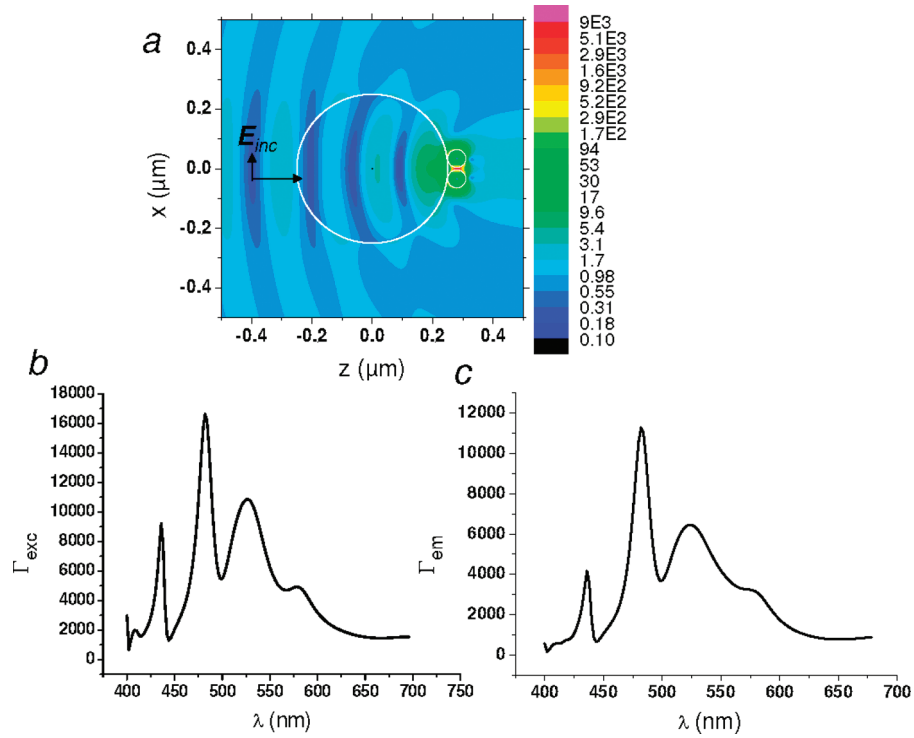

Figure 4. (a) Colored map of the electric field intensity enhancement at λ = 500 nm, (b) excitation rate enhancement, (c) emission rate enhancement as a function of the wavelength.

metallo-dielectric antenna, the two coupled metallic particles act as the feed element, and the chain of guiding metallic particles and reflector are simply replaced by a single dielectric sphere. The lack of a reflector in the proposed metallo-dielectric antenna seems surprising, but it should be mentioned that optical reflector elements so far have not provided clear benefits neither in the decay rate enhancements nor in the emission directionality. Moreover, as illustrated in Figure 2, the dielectric collector element is sufficiently performant to channel most of the emitted power without the need for an additional element contributing to the compactness of the antenna. Let us also emphasize that several nanofabrication techniques can potentially perform the challenging manufacturing of the proposed hybrid antenna.[6,24,42]

For the sake of completeness, we investigate the fluorescence enhancement of a molecule located in the vicinity of the nanoantenna. The fluorescence rate enhancement, Γ_{em}, can be defined as the product of the excitation rate, Γ_{exc}, and the quantum efficiency, η.[16,20] The excitation rate is defined as $|n_p \cdot E(r_p)|^2/|n_p \cdot E_0(r_p)|^2$, where n_p is the dipole direction and $E(r_p)$ and $E_0(r_p)$ are the local electric field at the dipole location r_p, respectively, with and without the antenna. The enhancement of the electric field intensity is displayed in Figure 4a when the antenna is illuminated at $\lambda = 500$ nm by a plane wave propagating along the *z*-axis. One observes a huge enhancement of light intensity in a nanometer sized volume delimited by the metallic spheres due to the combination of light focusing by the dielectric spheres with the excitation of coupled plasmons in the metallic dimer. This result was expected from Figure 1d and reciprocity[43,44] between the excitation and the radiative decay rates. Figure 4b displays very high excitation rates that can be strengthened by the excitation of WGM. This result stems from the high extinction cross section of the dielectric sphere, 10 times greater than the extinction cross section of the dimer of metallic nanoparticles at the plasmon resonance frequency. Consequently, this antenna presents all of the required properties for single molecular detection because both Γ_{exc} and η are highly enhanced and concurrent with a high directivity. This supposition is confirmed by a calculation of the fluorescence rate enhancement displayed in Figure 4c as a function of the excitation wavelength λ, where the excitation rates and quantum efficiencies are calculated with a wavelength shift of 20 nm, representative of common fluorophores, and Alexa dye in particular. One observes that fluorescence enhancements as high as 10^4 are achieved.

CONCLUSIONS

This study demonstrates that appropriately designed metallo-dielectric systems can serve as compact, highly directive and ultra radiative antennas. Let us emphasize that, contrary to fully metallic antennas, the high directivity of this antenna does not result from a plasmonic effect, and that it is efficient over a wide range of frequencies. As a consequence, the high directivity does compromise the high radiative decay rate enhancement offered by two coupled metallic particles,

and it is possible to exploit whispering gallery modes to further enhance the radiative decay rates. This work paves the way toward the design of compact, simple, and highly efficient optical antennas.

METHODS

Numerical simulations are performed within the framework of rigorous Mie theory combined with a multiple scattering formulation.[30−32] The single emitter is simulated as a dipolar source modeled by taking the first electric term in a multipole (Mie) expansion. The generalized Lorentz−Mie calculations are performed with a truncation order of $N = 20$ for the individual scatterers. Dielectric constants are obtained from tabulated data of the bulk material.[33,34]

The total emitted power, P_{tot}, and the radiative emitted power, P_{rad}, are calculated by integrating the radial component of the Poynting vector over a spherical surface surrounding the source at respective distances of 1 nm and 5 μm.

Acknowledgment. The authors thank Sebastien Bidault, Davy Gérard and Jérome Wenger for fruitful discussions.

REFERENCES AND NOTES

1. Mühlschlegel, P.; Eisler, H.-J.; Martin, O. J. F.; Hecht, B.; Pohl, D. W. Resonant Optical Antennas. *Science* **2005**, *308*, 1607–1609.
2. Bharadwaj, P.; Deutsch, B.; Novotny, L. Optical Antennas. *Adv. Opt. Photon.* **2009**, *1*, 438–483.
3. Tamaru, H.; Kuwata, H.; Miyazaki, H. T.; Miyano, K. Resonant Light Scattering from Individual Ag Nanoparticles and Particle Pairs. *Appl. Phys. Lett.* **2002**, *80*, 1826–1828.
4. Rechberger, W.; Hohenau, A.; Leitner, A.; Krenn, J. R.; Lamprecht, B.; Aussenegg, F. R. Optical Properties of Two Interacting Gold Nanoparticles. *Opt. Commun.* **2003**, *220*, 137–141.
5. Li, K.; Stockman, M. I.; Bergman, D. J. Self-Similar Chain of Metal Nanospheres as an Efficient Nanolens. *Phys. Rev. Lett.* **2003**, *91*, 227402.
6. Bidault, S.; García de Abajo, F. J.; Polman, A. Plasmon-Based Nanolenses Assembled on a Well-Defined DNA Template. *J. Am. Chem. Soc.* **2008**, *130*, 2750–2751.
7. Rigneault, H.; Capoulade, J.; Dintinger, J.; Wenger, J.; Bonod, N.; Popov, E.; Ebbesen, T. W.; Lenne, P. F. Enhancement of Single-Molecule Fluorescence Detection in Subwavelength Apertures. *Phys. Rev. Lett.* **2005**, *96*, 117401.
8. Popov, E.; Nevière, M.; Wenger, J.; Lenne, P. F.; Rigneault, H.; Chaumet, P.; Bonod, N.; Dintinger, J.; Ebbesen, T. Field Enhancement in Single Subwavelength Apertures. *J. Opt. Soc. Am. A* **2006**, *9*, 2342–2347.
9. Barnes, W. L. Fluorescence Near Interfaces: Role of Photonic Mode Density. *J. Mod. Opt.* **1998**, *45*, 661–669.
10. Farahani, J.; Pohl, D. W.; Eisler, H.-J.; Hecht, B. Single Quantum Dot Coupled to a Scanning Optical Antenna: A Tunable Superemitter. *Phys. Rev. Lett.* **2005**, *95*, 017402.
11. Rogobete, L.; Kaminski, F.; Agio, M.; Sandoghdar, V. Design of Plasmonic Nanoantennae for Enhancing Spontaneous Emission. *Opt. Lett.* **2007**, *32*, 1623–1625.
12. Thomas, M.; Greffet, J.-J.; Carminati, R.; Arias-Gonzales, J. R. Single-Molecule Spontaneous Emission Close to Absorbing Nanostructures. *Appl. Phys. Lett.* **2004**, *85*, 3863–3865.
13. Carminati, R.; Greffet, J.-J.; Henkel, C.; Vigoureux, J. M. Radiative and Non-radiative Decay of Single Molecule Close to a Metallic Nanoparticle. *Opt. Commun.* **2006**, *261*, 368–375.
14. Mertens, H.; Koenderink, A. F.; Polman, A. Plasmon-Enhanced Luminescence near Noble-Metal Nanospheres: Comparison of Exact Theory and an Improved Gersten and Nitzan Model. *Phy. Rev. B* **2007**, *76*, 115123.
15. Kaminski, F.; Sandoghdar, V.; Agio, M. Finite-Difference Time-Domain Modeling of Decay Rates in the Near Field of Metal Nanostructures. *J. Comput. Theor. Nanosci.* **2007**, *4*, 1–9.
16. Colas des Francs, G.; Bouhelier, A.; Finot, E.; Weeber, J. C.; Dereux, A.; Dujardin, E. Fluorescence Relaxation in the Near-Field of a Mesoscopic Metallic Particle: Distance Dependence and Role of Plasmon Modes. *Opt. Express* **2008**, *16*, 17654–17666.
17. Alù, A.; Engheta, N. Hertzian Plasmonic Nanodimer as an Efficient Nanoantenna. *Phys. Rev. B* **2008**, *78*, 195111.
18. Mirin, N. A.; Halas, N. J. Light-Bending Nanoparticles. *Nano Lett.* **2009**, *9*, 1255–1259.
19. Liaw, J.-W.; Chen, J.-S.; Chen, J.-H. Enhancement and Quenching Effect of Metallic Nanodimer on Spontaneous Emission. *J. Quant. Spectrosc. Radiat. Transfer* **2010**, *111*, 454–465.
20. Anger, P.; Bharadwaj, P.; Novotny, L. Enhancement and Quenching of Single-Molecule Fluorescence. *Phys. Rev. Lett.* **2006**, *96*, 113002.
21. Li, J.; Salindrino, A.; Engheta, N. Shaping Light Beams in the Nanometer Scale: A Yagi-Uda Nanoantenna in the Optical Domain. *Phy. Rev. B* **2007**, *76*, 245403.
22. Taminiau, T. H.; Stefani, F. D.; van Hulst, N. F. Enhanced Directional Excitation and Emission of Single Emitters by a Nano-Optical Yagi-Uda Antenna. *Opt. Express* **2008**, *16*, 16858–16866.
23. Koenderink, A. F. Plasmon Nanoparticle Array Waveguides for Single Photon and Single Plasmon Sources. *Nano Lett.* **2009**, *9*, 4228–4233.
24. Kosako, T.; Kadoya, Y.; Hofmann, H. F. Directional Control of Light by a Nano-Optical Yagi-Uda Antenna. *Nat. Photonics* **2010**, *4*, 312–315.
25. Pakizeh, T.; Käll, M. Unidirectional Ultracompact Optical Antennas. *Nano Lett.* **2009**, *9*, 2343–2349.
26. Soller, B. J.; Stuart, H. R.; Hall, D. G. Energy Transfer at Optical Frequencies to Silicon-on-Insulator Structures. *Opt. Lett.* **2001**, *26*, 1421–1423.
27. Schwartz, J. J.; Stavrakis, S.; Quake, S. R. Colloidal Lenses Allow High-Temperature Single-Molecule Imaging and Improve Fluorophore Photostability. *Nat. Nanotechnol.* **2009**, *5*, 127–132.
28. Gérard, D.; Devilez, A.; Aouani, H.; Stout, B.; Bonod, N.; Wenger, J.; Popov, E.; Rigneault, H. Efficient Excitation and Collection of Single Molecule Fluorescence Close to a Dielectric Microspheres. *J. Opt. Soc. Am. B* **2009**, *26*, 1473–1478.
29. Pellegrini, G.; Mattei, G.; Mazzoldi, P. Light Extraction with Dielectric Nanoantenna Arrays. *ACS Nano* **2009**, *3*, 2715–2721.
30. Stout, B.; Auger, J. C.; Devilez, A. Recursive T-Matrix Algorithm for Resonant Multiple Scattering: Applications to Localized Plasmon Excitation. *J. Opt. Soc. Am. A* **2008**, *25*, 2549–2557.
31. Lax, M. Multiple Scattering of Waves. *Rev. Mod. Phys.* **1951**, *23*, 287–310.
32. Wiscombe, W. J. Improving Mie Scattering Algorithms. *Appl. Opt.* **1980**, *19*, 1505–1509.
33. Yamada, Y.; Uyama, H.; Watanabe, S.; Nozoye, H. Deposition at Low Substrate Temperatures of High-Quality TiO_2 Films by Radical Beam-Assisted Evaporation. *Appl. Opt.* **1999**, *38*, 6638–6641.
34. Palik, E. D. *Handbook of Optical Constants of Solids*; Academic Press: New York:, 1985.
35. Koyama, K.; Yishita, M.; Baba, M.; Suemoto, T.; Akiyama, H. High Collection Efficiency in Fluorescence Microscopy with a Solid Immersion Lens. *Appl. Phys. Lett.* **1999**, *75*, 1667–1669.
36. Gérard, D.; Wenger, J.; Devilez, A.; Gachet, D.; Stout, B.; Bonod, N.; Popov, E.; Rigneault, H. Strong Electromagnetic Confinement near Dielectric Microspheres to Enhance

Single-Molecule Fluorescence. *Opt. Express* **2008**, *16*, 15297–15303.
37. Devilez, A.; Bonod, N.; Wenger, J.; Gérard, D.; Stout, B.; Rigneault, H.; Popov, E. Three-Dimensional Subwavelength Confinement of Light With Dielectric Microspheres. *Opt. Express* **2009**, *17*, 2089–2094.
38. Johnson, B. R. Theory of Morphology-Dependent Resonances: Shape Resonances and Width Formulas. *J. Opt. Soc. Am. A* **1993**, *10*, 343–352.
39. Gorodetsky, M. L.; Savchenkov, A. A.; Ilchenko, V. S. Ultimate Q Optical Microsphere Resonator. *Opt. Lett.* **1996**, *21*, 453–455.
40. Ringler, M.; Schwemer, A.; Wunderlich, M.; Nichtl, A.; Kürzinger, K.; Klar, T. A.; Feldmann, J. Shaping Emission Spectra of Fluorescent Molecules with Single Plasmonic Nanoresonators. *Phys. Rev. Lett.* **2008**, *100*, 203002.
41. Kinkhabwala, A.; Yu, Z.; Fan, S.; Avlasevich, Y.; Müllen, K.; Moerner, W. E. Large Single-Molecule Fluorescence Enhancements Produced by a Bowtie Nanoantenna. *Nat. Photonics* **2009**, *3*, 654–657.
42. Merlein, J.; Kahl, M.; Zuschlag, A.; Sell, A.; Halm, A.; Boneberg, J.; Leiderer, P.; Leitenstorfer, A.; Bratschitsch, R. Nanomechanical Control of an Optical Antenna. *Nat. Photonics* **2008**, *2*, 230–233.
43. Carminati, R.; Nieto-Vesperinas, M.; Greffet, J.-J. Reciprocity of Evanescent Electromagnetic Waves. *J. Opt. Soc. Am. A* **1998**, *15*, 706–712.
44. Bharadwaj, P.; Novotny, L. Spectral Dependence of Single Molecule Fluorescence Enhancement. *Opt. Express* **2007**, *15*, 14266–14274.